THE UNIVERSITY of EDINBURGH

Edinburgh Research Explorer

Hydrogen-isotope systematics in degassing basaltic magma and application to Indonesian arc basalts

OPEN ACCESS

Hydrogen-isotope systematics in degassing basaltic magmand application to Indonesian arc basalts

JAN C. M. DE HOOG [1, 2] ✉

BRUCE E. TAYLOR [3]

MANFED J. VAN BERGEN [2]

[1] Dept. of Earth Sciences, University of Oxford, Parks Road, Oxford OX1 3PR, United Kingdom

[2] Department of Earth Sciences, Utrecht University, P.O. Box 80021, 3508 TA Utrecht, The Netherlands

[3] Geological Survey of Canada, 601 Booth Street, Ottawa, Ontario, K1A 0E8, Canada

Revised manuscript for

Chemical Geology

Isotope Geoscience Section

9 July 2013

✉ Corresponding author, email: cees-jan@earth.ox.ac.uk

Tel +44-1865-282113

Fax +44-1865-272072

Abstract

We have developed a predictive model for hydrogen-isotope shifts during degassing of basaltic-andesitic magma that takes the variation of water species with water content and temperature into account. OH* (water dissolved as hydroxyl) is the dominant dissolved water species for the range of naturally observed magmatic water contents (0-8 wt.%) and temperatures (>800°C), and increases in importance with higher temperatures and lower water contents. We used our hydrogen fractionation model and published experimental data to derive values for hydrogen isotope fractionation factors between melt and H_2O vapor of $10^3 \ln \alpha_{OH*} = 34.9 + 16.7 \times 10^6/T^2$ for OH* and $10^3 \ln \alpha_{H_2O*} = -30.3 + 16.7 \times 10^6/T^2$ for H_2O* (water dissolved as molecular water). A value of zero for the latter, as was assumed in some recent and earlier studies, is incompatible with our model results. As a consequence of the progressively increasing OH*/H_2O* ratio in the melt during degassing, the bulk hydrogen fractionation factor also increases continuously. In contrast, the influence of temperature on the bulk fractionation factor $\Delta D_{vapor-melt}$ is relatively small.

We applied the hydrogen fractionation model to thirty subaerial lavas of basaltic composition from eight volcanoes located in the Indonesian arc system. All samples are extensively degassed, as average contents of residual water in the melt are only ~0.15 wt.%. Whole-rock δD values range from -109‰ to -57‰ VSMOW (average = -89‰). Oxygen isotope compositions of the same samples range from +5.3‰ to +6.7‰ VSMOW and are close to MORB values, indicating that crustal contamination or post-eruptive weathering was insignificant. Hydrogen isotopes fractionated markedly during degassing, and our data agree best with dominantly closed-system exsolution of magmatic water during magma ascent and storage, followed by syn-eruptive open-system degassing at depths of less than a few hundred meters. Magmatic water was derived from a mantle source with a typical D-enriched arc isotopic signature. Within-suite systematics suggest variations in initial δD and $\delta^{18}O$ values for some volcanic centers.

1. Introduction

Hydrogen isotope compositions of igneous rocks and fluids have been used to explore sources of magmatic water, the water cycle in subduction zones, the degassing history of lavas, and fluid-rock interaction (e.g., Kyser and O'Neill, 1984; Poreda, 1985; Taylor, 1986; Giggenbach, 1992; Nadeau et al., 1993; Pineau et al., 1999; Shaw et al., 2008). A key aspect in studies of magmatic systems is the extent to which primary isotopic characteristics are influenced by fractionation during degassing. Previous work on degassing has focused mainly on rocks of dacitic to rhyolitic composition (e.g., Taylor et al., 1983; Newman et al., 1988; Wilding et al., 1993; Kusakabe et al., 1999), whereas only few studies have addressed the hydrogen isotope systematics of basaltic and andesitic rocks, particularly in arc settings (e.g., Taran et al., 1997; Pineau et al., 1999; Shaw et al., 2008). Insights into the degassing history of basaltic magmas is of particular importance to research on eruptive products that concentrates on petrogenetic processes affecting magma sources in the mantle wherein volatiles are involved.

Here we present new hydrogen isotope data, supported by oxygen isotope results, on mafic rocks from active volcanoes in Indonesia. In order to interpret the isotopic signatures, hydrogen fractionation during volatile exsolution must be accounted for, as the samples represent advanced stages of degassing. Hydrogen isotope fractionation between magma and exsolved vapor is not constant but depends on the water content of the melt (Taylor, 1986; Pineau et al., 1998), which changes progressively during degassing of a magma batch in response to depressurization and crystallization. Currently, no model is available that takes shifting fractionation factors during degassing into account. Also, uncertainty about fractionation factors still exists (e.g., Shaw et al., 2008). To accommodate the need for an improved hydrogen fraction model, we combine published experimental bulk vapor-melt fractionation factors with published water speciation models to calibrate an internally consistent model that predicts vapor-melt fractionation factors for basaltic to basaltic andesite magma as a function of water content and temperature. The hydrogen-isotope degassing model is used to determine degassing characteristics of subduction-related basaltic volcanism in Indonesia and to pose constraints on the sources of magmatic water.

2. Hydrogen isotope-fractionation during degassing

The relative amounts of dissolved molecular and hydroxyl water in silicate melts vary with total water concentration, temperature and probably melt composition (e.g., Stolper, 1982a, b, 1989; Silver and Stolper, 1989; Silver et al., 1990; Ihinger et al., 1999), and fractionation factors depend on temperature and melt composition (Taylor, 1986; Dobson et al., 1989). Therefore, the systematics of hydrogen isotope fractionation during degassing of magmas are not straightforward and have commonly been approximated by a constant value in the literature. Vapor-melt fractionation factors have been determined for siliceous melts in a number of experiments (*e.g.*, Kuroda et al., 1982; Taylor and Westrich, 1985; Dobson et al., 1989), but very few studies involved magmas of basaltic or andesitic composition (Pineau et al., 1998). Precise modeling of the hydrogen isotope shift during degassing requires further integration of both water speciation and hydrogen fractionation data. Current data on water speciation and hydrogen isotope fractionation can be used to develop an integrated isotopic degassing model for magmas of basaltic to andesitic composition as a function of total water content and temperature.

2.1. Isotopic composition and speciation of water in silicate melts

Water dissolves in silicate melts as molecular water (referred to as H_2O*) and hydroxyl (referred to as $OH*$) groups (Stolper, 1982b), which have different isotopic compositions. The bulk hydrogen isotope composition[1] of the melt can be expressed by:

$$\delta D_{H_2O \text{ dissolved}} = Y_{H_2O*} \times \delta D_{H_2O*} + [1 - Y_{H_2O*}] \times \delta D_{OH*} \qquad [1]$$

where Y_{H_2O*} is the fraction of total dissolved water present as molecular water in the melt (Taylor, 1986). δD_i is the hydrogen isotope composition of each component *i*.

Similarly, the bulk hydrogen isotope fractionation between water vapor (H_2O) and melt ($\Delta D_{vapor-melt}$) is a function of the relative amounts of hydroxyl and molecular water in the melt and the fractionation factor relative to H_2O vapor for each species:

---

[1] $\delta D = [((D/H)_{sample} / (D/H)_{standard}) - 1] \times 10^3$ permil

$$\Delta D_{vapor\text{-}melt} = Y_{H_2O*} \times \Delta D_{vapor\text{-}H_2O*} + [1\text{-}Y_{H_2O*}] \times \Delta D_{vapor\text{-}OH*} \qquad [2]$$

where $\Delta D_{vapor\text{-}melt} = \delta D_{vapor} - \delta D_{melt}$, $\Delta D_{vapor\text{-}H_2O*} = \delta D_{vapor} - \delta D_{H_2O*}$, and $\Delta D_{vapor\text{-}OH*} = \delta D_{vapor} - \delta D_{OH*}$ (Holloway and Blank, 1994).

2.2. Water dissolution model

Early water-solubility models assumed that water dissolves solely as hydroxyl (OH*) species in silicate melts, but spectroscopic measurements have shown that molecular water (H_2O*) is present at higher dissolved water content (see Stolper, 1982b, for an overview). The solubility mechanism of water in silicate melts is still debated (e.g., Zeng et al., 2000; Schmidt et al., 2000), mainly because the determination of water species is hampered by experimental and analytical difficulties. Early water speciation measurements were conducted on quenched soda-lime glasses that were assumed to represent water speciation in melts (Stolper, 1982a, 1989; Silver and Stolper, 1989; Silver et al., 1990). However, the relaxation of water species is faster than quench rates, thus the water speciation observed in glasses represents conditions at the glass-transition temperature (T_g; Dingwell and Webb, 1990) and early speciation results are now deemed inaccurate (Zhang et al., 1995). Subsequent in-situ measurements on hydrous melts (Nowak and Behrens, 1995; Shen and Keppler, 1995) showed much higher fractions of OH* at high temperature compared to earlier studies on quenched glass. However, quenched-glass experiments shown to be unaffected by re-equilibration of water speciation suggested calibration difficulties of IR spectroscopy signals from in-situ experiments (Ihinger et al., 1999). More recent work shows that, with careful calibration, consistent results can be obtained from both in-situ and quenched glass methods, the latter being more precise (Withers et al., 1999; Behrens and Nowak, 2003; Liu et al., 2004; Hui et al., 2008).

2.2.1. Water speciation and water concentration

Water dissolves in silicate melt as OH* and H_2O* species; the latter becomes increasingly important above 0.2 wt.% dissolved water and dominates water speciation above a few weight percent dissolved water (Stolper, 1982b; Zhang, 1999). The equilibrium constant of a

(simplified) water-melt solution reaction, $H_2O^*(melt) + O(melt) = 2OH^*(melt)$, can be expressed as:

$$K = (X_{OH^*})^2 / (X_{H_2O^*} \times X_O) \qquad [3]$$

where X_{OH^*}, $X_{H_2O^*}$ and X_O refer, respectively, to the mole fraction of hydroxyl groups, molecular water and bridging oxygens in the melt (Stolper, 1982b). The total water content at which H_2O^* becomes dominant over OH^* is temperature dependent. Ihinger et al. (1999) calibrated the temperature dependence of the equilibrium constant K in rhyolite glasses as:

$$\ln K = 1.89 \pm 0.05 - \frac{3120 \pm 40}{T} \qquad [4]$$

with T in Kelvin. In most natural systems (>750°C, <7 wt.% H_2O) OH^* is the dominant species. K is independent of the amount of dissolved water because the model assumes ideal mixing between water and melt. In reality, K will vary with water concentration and can be approximated by a regular solution model (Stolper, 1989; Ihinger et al., 1999), which requires iterative methods to calculate water speciation from total water content and temperature. However, Zhang et al. (1997) and Ihinger et al. (1999)showed water speciation in rhyolitic melts to be approximately ideal at total water contents at least up to 2.4 wt.%. Model calculations show that deviations from ideal mixing become increasingly less important at temperatures and water contents applicable to degassing of basaltic and andesitic magmas (**Fig. 1**). Therefore, we use ideal mixing of dissolved water species in our hydrogen fractionation model (Section 2.4.).

A small pressure dependence of water speciation in rhyolites has recently been demonstrated by Hui et al. (2008) at pressure over 1 GPa, but since magmatic degassing occurs at lower pressures this will be ignored in our hydrogen isotope fractionation model.

2.2.2. Compositional dependence

Water speciation studies have mostly been applied to silica-rich systems (e.g., Ihinger et al., 1999; Nowak and Behrens, 1995; Shen and Keppler, 1995; Liu et al., 2004). Only limited reliable data are available for andesitic and basaltic compositions (Ohlhorst et al., 2001; Botcharnikov et al., 2006), so composition dependence of water speciation is a field that needs

further study. Ihinger et al. (1999) reported a slight compositional dependence for water speciation; haplogranitic melts showed OH enrichments of 5-10% relative to concentrations in rhyolite. Recently, Botcharnikov et al. (2006) concluded that water speciation changes little from andesite to rhyolite. They derive a relationship for ln K in andesitic melts that leads to a higher amount of OH* for a given water content than the equation of Ihinger et al. (1999). It is unclear whether this is a compositional effect, as the results by Botcharnikov et al. (2006) are about an order of magnitude less precise than those of Ihinger et al. (1999). In the absence of conclusive evidence that would allow a robust quantification of compositional effects, our hydrogen fractionation model assumes that water speciation in basaltic melts can be approximated by that in rhyolitic melts (Eq. 4). Our model can easily be adapted if more conclusive data on water speciation in basaltic melts becomes available.

2.3. Vapor-melt fractionation factors

2.3.1. Temperature dependence

Fractionation factors and their temperature dependence for hydrogen isotopes have been determined for various hydrous minerals (summarized in Taylor, 1986). Relatively few data on fractionation in the system silicate melt-aqueous fluid have been published, mainly due to experimental difficulties (Dobson et al., 1989). Bulk fractionation factors α [2] were found to be 1.020-1.024 at 950°C and 2.3-3.0 wt.% H_2O in rhyolite melt (Taylor and Westrich, 1985). Richet et al. (1986) found $\alpha=1.025$ for sodium aluminosilicate melt at temperatures between 870 and 1250ºC at 2 kbar (~5.4 wt. H_2O), but reported hydrogen loss in the vessel. Dobson et al. (1989) determined fractionation factors of rhyolitic and feldspathic glasses with very low water contents (<0.2 wt.%) in which nearly all dissolved water is present as hydroxyl (OH*). Vapor-OH* fractionation factors decrease from 1.051 to 1.040 for rhyolitic glass and from 1.049 to 1.035 for feldspathic glass as temperature increases from 530 to 750ºC. The temperature dependence can be described by:

---

[2] $\alpha_{v-m} = (\delta_v + 1000) / (\delta_m + 1000)$ and $\Delta D_{v-m} = \delta_v - \delta_m = (\alpha_{v-m} - 1) / (\delta_m + 1000) \approx 10^3 \ln \alpha_{v-m}$

$$10^3 \ln \alpha_{\text{vapor-OH*}} = a + b/T^2 \qquad\qquad\qquad [5]$$

where T is expressed in Kelvin, and a and b are constants to be determined for the system of interest (Dobson et al., 1989). Differences in a between rhyolitic obsidian ($a \approx 23$) and feldspathic glass ($a \approx 15$) indicate that the fractionation factor varies with glass composition. However, the temperature dependence b is rather constant for a given composition, resulting in approximately parallel lines when $10^3 \ln \alpha$ is plotted against T^{-2} (Dobson et al., 1989) (**Fig. 2**). Given the lack of experimental data in basaltic and andesitic systems, we assume in our model that the temperature dependence of fractionation factors is similar to that inferred for rhyolites.

2.3.2. Compositional dependence

To determine a for basaltic-andesitic systems, we need to know the vapor-OH* fractionation factor ($\alpha_{\text{vapor-OH*}}$) at given temperature. Using a value of 39.3‰ for $\Delta D_{\text{vapor-melt}}$ determined on a submarine glassy lava with 0.5 wt.% dissolved water (Pineau et al., 1998), we derive a value of $10^3 \ln \alpha_{\text{vapor-OH*}} = 42.2$‰ at 1250°C, after correction for a small amount of molecular water (0.02 wt.%). As mentioned above, the temperature dependence of $10^3 \ln \alpha_{\text{vapor-OH*}}$ is unknown, but as obsidian and hydrous minerals show nearly parallel trends in $10^3 \ln \alpha - 1/T$ space, we infer that the trend for basaltic melt is probably close to rhyolitic melt. Combining the value of $10^3 \ln \alpha_{\text{vapor-OH*}}$ at 1250°C with the slope of the rhyolite fractionation line, we derive the following equation for the hydrogen isotope fractionation between vapor and OH* in basaltic-andesitic melt:

$$10^3 \ln \alpha_{\text{vapor-OH*}} = 35.0 + 16.7 \times 10^6/T^2 \qquad\qquad [6]$$

with T in Kelvin (**Fig. 2**).

2.3.3. Variation with water content

According to D/H fractionation experiments in basaltic andesite at 1250°C, the bulk fractionation factor ($\Delta D_{\text{vapor-melt}}$) decreases from 32‰ to 20‰ for 0.5 to 3 kbar, equivalent to a total water content of 2.3 and 7.0 wt.%, respectively (Pineau et al., 1998). This change reflects a shift in water speciation, $i.e.$, an increase in H_2O* at the expense of OH* with increasing water content. It has been suggested that $\alpha_{\text{vapor-}H_2O*}$ is close to unity, as there will

8

be only little difference in the chemical affinity of molecular water in the melt and water vapor (Taylor, 1986; Dobson et al., 1989), and this rationale has been adopted in recent literature (Shaw et al., 2008). Using $\alpha_{vapor-OH*} = 1.043$ (from $10^3 \ln \alpha_{vapor-OH*} = 42.1‰$), assuming $\alpha_{vapor-H_2O*} = 1$, and calculating water speciation from Eq. 4 at 1250°C, we can determine the relation between the bulk fractionation factor $\alpha_{vapor-melt}$ and total dissolved water by substituting these values in Eq. 2. However, using this value for $\alpha_{vapor-H_2O*}$ our model (**Fig. 3)** predicts a much smaller decrease of $\Delta D_{vapor-melt}$ with increasing water content than indicated by data from Pineau et al. (1998). This discrepancy suggests that either (1) the assumption $\alpha_{vapor-H_2O*} = 1$ is invalid; or (2) the water speciation model overestimates the amount of hydroxyl groups in the melt. Recent studies of water speciation (Nowak and Behrens, 2001; Botcharnikov et al., 2006) predicts values of OH* that are not significantly different than the model of Ihinger et al. (1999), and it is therefore unlikely that the model significantly overestimates the amount of OH*. We also observe that varying the value for K in the ideal mixing model (Eq. 4), which would correspond to a compositional dependence of water speciation, does not reproduce the curve from Pineau et al. (1998). Therefore, we follow the suggestion of Pineau et al. (1998) that the fractionation factor for molecular water in basaltic andesite deviates from unity.

A study by Newman et al. (1988) refers to a value of $\alpha_{vapor-H_2O*} = 0.9857$ (and $\alpha_{vapor-OH*} = 1.052$) in their degassing model of Mono Craters obsidians (California, USA), but the authors do not provide a rationale for the choice of these values. Pineau et al. (1998) determined a value of 1.016 for the fractionation factor at infinite water concentration (when $H_2O* \gg OH*$) by inferring a linear correlation between $\Delta D_{vapor-melt}$ and $1/\sqrt{(H_2O_{total})}$. However, our model predicts that this relationship is non-linear, a feature that can also be observed in the experimental D/H fractionation data of Pineau et al. (1998), although it was obscured by data from natural basalt and phonolite samples the authors included.

Therefore, we performed a best-fit calculation to determine values of $\alpha_{vapor-OH*}$ and $\alpha_{vapor-H_2O*}$ using the water speciation model described in Eq. 4 at 1250°C, the experimental data of Pineau et al. (1998), and Eq.2. Values of $\alpha_{vapor-H_2O*} = 0.9775$ and $\alpha_{vapor-OH*} = 1.0431$ at 1250°C combine to comprise a bulk fractionation factor that is in good agreement with the

9

results of Pineau et al. (1998) (**Fig. 3**). Analogous to $\alpha_{vapor\text{-}OH*}$, the temperature dependence of $\alpha_{vapor\text{-}H_2O*}$ can be expressed as:

$$10^3 \ln \alpha_{vapor\text{-}H_2O*} = {}^-29.9 + 16.7 \times 10^6 / T^2 \qquad [7]$$

Interestingly, the difference between $10^3 \ln \alpha_{vapor\text{-}OH*}$ and $10^3 \ln \alpha_{vapor\text{-}H_2O*}$ in rhyolite (65.1; Newman et al., 1988) is nearly the same as the difference in our values (64.9), which suggests that this difference is relatively insensitive to variations in magma composition. Hence, bulk fractionation factors determined at low water contents ($<$0.2 wt.%, containing exclusively OH*) may be used to approximate $10^3 \ln \alpha_{vapor\text{-}H_2O*}$ for any magma composition with the expression:

$$10^3 \ln \alpha_{vapor\text{-}H_2O*} = 10^3 \ln \alpha_{vapor\text{-}OH*} - 65 \qquad [8]$$

2.3.4. Pressure dependence

From theoretical considerations it can be predicted that mineral-vapor fractionation will be pressure dependent, being most pronounced near the critical temperature of water at 376°C (Driesner, 1997). Experiments have demonstrated that D/H fractionation between water and brucite increases linearly by 12.4‰ as vapor density increases from 0.07 to 1.035 g/cm^3 at 380°C (Horita et al., 1999). However, such pressure effects are probably negligible at the high temperatures prevailing in magmatic systems (Driesner, 1997), apart from for the obvious effect on water solubility that leads to vapor-melt saturation and degassing. We wish to point out that our model is independent of water solubility models as it relates the hydrogen isotope fractionation factor to the water content of the melt, not to pressure. It is therefore also independent of the fluid composition, as a reduced water activity in the fluid will not change water speciation or isotopic composition of the melt in equilibrium with that fluid.

2.4. Hydrogen isotope fractionation model

2.4.1. Bulk fractionation factor

The bulk fractionation factor can be calculated for given temperature, water concentration

of the melt and melt bulk composition. First, the water concentration is expressed in mole
fractions on a single oxygen basis (following Silver et al., 1990):

$$X_w = \frac{C_{H_2O}/18.015}{C_{H_2O}/18.015 + (100 - C_{H_2O})/M_O}$$ [9]

where C_{H_2O} is the total water concentration in the melt and $M_O = 100/\sum_i \left(C^i/M^i\right)$, with C^i the

anhydrous concentration of component i with the concentrations of all components normalized
to 100 wt.% and M^i the molecular weight of component i on a single oxygen basis.

Given $X_O = 1 - X_w - 0.5X_{OH*}$ and $X_{H_2O*} = X_w - 0.5X_{OH*}$ (Silver et al., 1990), then

$$K = \frac{(X_{OH*}^{melt})^2}{(X_{H_2O*}^{melt} \times X_O^{melt})} = \frac{(X_{OH*}^{melt})^2}{(X_w - \frac{1}{2}X_{OH*}^{melt})(1 - X_w - \frac{1}{2}X_{OH*}^{melt})}$$ [10]

(*cf*. Eq. 3; after Stolper, 1982b). X_{OH*} can be solved for given T:

$$X_{OH*} = \frac{-b - \sqrt{b^2 - 4ac}}{2a}$$ [11]

with $a = K/4 - 1$, $b = -K/2$, $c = K \times (X_w - X_w^2)$ and $\ln K = 1.89 - \dfrac{3120}{T}$ (*cf*. Eq. 4; after Ihinger et
al., 1999).

Bulk hydrogen isotope fractionation between melt and vapor can now be calculated for given
water content and temperature by rewriting Eq. 2:

$$\Delta D_{vapor-melt} = \Delta D_{vapor-H_2O*} + (1 - Y_{H_2O*}) \times (\Delta D_{v-OH*} - \Delta D_{v-H_2O*})$$ [12]

with $\Delta D_{v-OH*} = 35.0 + 16.7 \times 10^6/T^2$ (*cf*. Eq. 6), $\Delta D_{v-H_2O*} = -29.9 + 16.7 \times 10^6/T^2$ (cf. Eq. 7)
and $Y_{H_2O*} = X_{H_2O*}/X_w = [1 - X_{OH*}/2]/X_w$.

   The temperature dependence of hydrogen isotope fractionation between vapor and melt
($\Delta D_{vapor-melt}$) with total water content in the melt is rather small (Fig. 3) and insignificant for a
large range of temperatures and water contents in natural systems. A temperature independent
relation that approximates $\Delta D_{vapor-melt}$ can be expressed as follows:

$$\Delta D_{vapor-melt} (‰) = 44.53 \times (C_{H_2O}/7.03 + 1)^{-1.2}$$ [13]

where C_{H_2O} is the total water concentration of the melt in wt.%. For a temperature range of 900
to 1250°C, this equation predicts $\Delta D_{vapor-melt}$ within 1‰ at 1-7 wt.% H_2O, and within 2.5‰ at

11

less than 1 wt.% H_2O. If higher precision is needed Eq. 12 should be used.

The fractionation factor α can be calculated using the formula

$$\alpha_{v-m} = 1 + [\Delta D_{vapor-melt} / (\delta D_{melt} + 1000)] \tag{14}$$

The approximations $\Delta D_{vapor-melt} \approx 10^3 \ln \alpha_{v-m}$ and $\delta D_{melt} = 0‰$ that are commonly used in other stable isotope systems leads to significant deviations for the large fractionations associated with water contents common in magmatic systems.

2.4.2. Degassing models

From the bulk fractionation factor α and δD_{melt}, the δD value of the exsolving vapor phase can be calculated from:

$$10^3 \ln \alpha_{vapor-melt} = 1000 \times [\ln (1 + \delta D_{vapor} / 1000) - \ln (1 + \delta D_{melt} / 1000)] \tag{15}$$

(Taylor, 1986), which can be rearranged to

$$\delta D_{vapor} = \alpha_{vapor-melt} \times (1000 + \delta D_{melt}) - 1000 \tag{16}$$

The δD value of the melt after a fraction $(1-F)$ of vapor has been removed with continuous isotopic re-equilibration between the fluid phase and the melt (closed-system vapor separation) is described by:

$$\delta D_{melt} = \delta D_i - (1 - F) \times 1000 \ln \alpha \text{ (Taylor, 1986)} \tag{17}$$

where δD_i is the initial hydrogen isotopic composition of the melt, and F is the fraction of water remaining dissolved in the melt. The maximum isotopic shift of the residual magma upon vapor exsolution is, in this case, limited to the fractionation between the vapor and the melt phase (in permil).

The δD value of the melt during open-system vapor separation, when exsolving equilibrium vapor is instantaneously removed from the melt without further isotopic re-equilibration, is formulated as:

$$\delta D_{melt} = \delta D_i - (1000 + \delta D_i) \times (1 - F^{\alpha - 1}) \text{ (Taylor, 1986)} \tag{18}$$

The approximation $\delta D_i = 0‰$ would lead to significant inaccuracies of more than 5‰ in calculation of δD_{melt} if δD_i is substantially different from zero (Taylor, 1986) (e.g., $>$5‰ for $F = 0.1$ with $\delta D_i = -70‰$), as is common to many magmas.

12

2.4.3 Applicability and model evaluation

Since the relative amounts of molecular water and hydroxyl groups vary with the total amount of dissolved water (and thus with *F*), the bulk fractionation factor α changes as degassing progresses. For closed-system degassing the calculated fractionation factor for the water content of the residual melt corresponding to the chosen extent of degassing can be used. In contrast, during open-system degassing, vapor exsolves with an instantaneous δD value determined by the progressively changing melt-vapor fractionation factor at the moment of separation from the melt. Throughout degassing, vapor and melt change in hydrogen isotope composition, and their δD values can be estimated by modeling small incremental steps of water exsolution.

The hydrogen isotope compositions of vapor and melt, at any given point in the degassing scenario, not only depend on the fraction of vapor lost, but also on the initial water concentration. The effects of progressively changing fractionation factors during magma degassing, as detailed in our model described above, are illustrated in **Fig. 4**. For comparison, the changes in δD_{melt} using initial and final fractionation factors (at the start and at the end of degassing, respectively) have been indicated as well. The model curves for progressively changing fractionation factors lie between these extremes.

To make conclusions about degassing processes based on hydrogen isotope data we need to evaluate its sensitivity to input variables (P, T, water content) and external factors (e.g., gas composition). These variables may have different influences for the two end-member degassing modes.

Uncertainties in the model related to the lack of water speciation data for basaltic melts appears to be limited. When we use speciation data for andesite (Botcharnikov et al., 2006) to derive values for $\Delta D_{v\text{-}OH*}$ □ and $\Delta D_{v\text{-}H_2O*}$, the effect on δD_{melt} is within 2‰ over the whole degassing range (1-6 wt.% H_2O) for closed as well as open-system degassing. The reason for this small effect is that most of degassing takes place at low water contents, when most water is dissolved as OH*, and the value of $\Delta D_{v\text{-}OH*}$ □ is well constrained by experimental data of Pineau et al. (1998). The same counts for the temperature dependence of $\Delta D_{v\text{-}OH*}$ □ and $\Delta D_{v\text{-}H_2O*}$, which are now assumed to be similar to rhyolite. If we take the temperature of albite melt (Dobson et al.,

1989), which has a stronger temperature dependence close to that of mineral-vapor data, the maximum deviation of δD_{melt} is only 1‰. We therefore conclude that despite the uncertainties in extrapolation low-temperature water speciation data from rhyolites to high-temperature basalts, the effect on degassing models is comparable to uncertainty of δD measurements. Larger uncertainties arise from estimates of initial water contents and δD_{melt} values. For closed system degassing, differences in initial water contents result in relatively small differences of <5‰ in samples that are degassed to <1 wt.% water (Fig. 4). Differences in hydrogen isotope composition therefore dominantly reflect differences in initial composition. For open-system degassing no such inference can be made. Increasing the water content by a factor two has a similar effect as a lower initial isotopic composition of ca. 15‰ (Fig. 4).

The CO_2 content of the melt has an important effect on water solubility, and the presence of CO_2 will increase the pressure at which water will start to exsolve from the melt. However, the speciation of water is pressure independent at P<10 kbar and the presence of CO_2 does not affect ΔD_{v-m} or any of the modeling results presented above.

Temperature effects on δD_{melt} values are negligible above 900°C due to the counteracting effects of temperature on water speciation and $\Delta D_{v-OH*}\square$ and ΔD_{v-H_2O*} (see Section 2.4.1 and Fig. 3).

3. Hydrogen and oxygen isotope systematics of Indonesian basalts

The degassing history of volcanic material is important to estimate isotopic shifts during degassing, e.g., when primary isotopic signals are being studied (e.g., Gerlach and Taylor, 1990; Aubaud et al., 2005; De Hoog et al., 2001) or the influence of meteoric water is evaluated (e.g., Taylor et al., 1983). In addition, the style of degassing plays an important role in fractionating different volatiles relative to each other, which needs to be evaluated for correct interpretation of temporal changes in volcanic gases (e.g., Burton et al., 2007).

Here we present new hydrogen and oxygen isotope data of basalts from the Indonesian arc system. The results will be discussed in terms of degassing characteristics of basaltic magmas and the origin and isotopic identity of magmatic water, applying the hydrogen fractionation

model developed in Section 2.

3.1. Sample description

Samples were collected from seven volcanoes along the Sunda and Sangihe arcs in Indonesia (**Fig. 5)**, which have been described in detail in De Hoog et al. (2001) and Hoogewerff (1999). With the exception of one air-fall tephra (Boleng, sample 34-8), all samples are from subaerial lavas. The samples represent recently erupted products; those from Batur, Rinjani, Krakatau and Soputan were erupted within the last two centuries. Two samples from each volcano were analyzed for hydrogen isotopes, except for Soputan and Batur, from which 8 and 10 samples were collected, respectively, to detect possible within-suite systematics. A single sample was analyzed from Krakatau. The samples are fresh, with no visible signs of alteration, are glassy, and contain 15-30 modal% phenocrysts consisting of olivine, clinopyroxene and plagioclase, occasionally accompanied by magnetite and orthopyroxene. Hydrous minerals are virtually absent. Chemical compositions range from basaltic to basaltic-andesite (49-57 wt.% SiO_2) and from low to high-K.

3.2. Analytical methods

Hydrogen isotope compositions were determined on powdered whole-rock samples. About 1 g of powder was degassed overnight at 150°C under vacuum, prior to extraction using a uranium reduction method similar to that of Bigeleisen et al. (1952). Measured δD values were normalized to a VSMOW-SLAP scale, which accounts for H_3^+ correction and for scale expansion. The H_2O content of each sample was determined from the manometrically measured yield of H_2 released during the hydrogen extraction technique. The uncertainty of reported values of δD_{VSMOW} is ca. 2‰, and the uncertainty of H_2O contents is ca. 0.02 wt.%.

Oxygen isotope analysis of whole-rock samples was carried out following a procedure similar to that of Clayton and Mayeda (1963), in which oxygen is extracted from rock powder by reaction with BrF_5. The uncertainty in reported values of $\delta^{18}O_{VSMOW}$ is ± 0.2‰. Our

average value of $\delta^{18}O$ for NBS-28 quartz of +9.5±0.2‰ is within analytical precision of the recommended value of 9.66‰.

3.3. Results

3.3.1. Hydrogen isotope compositions and water contents

Whole-rock δD values show a wide range, from -109 to -57‰, but most values fall between -100 and -80‰, and average -89‰ (**Table 1**). Averages of the larger sample sets from Batur (-92±6‰) and Soputan (-88±6‰) do not differ significantly from the overall average. Large ranges of δD values from degassed lavas and dikes have been previously reported in the literature (-125 to -45‰; Taylor et al., 1983; Newman et al., 1988; Anderson and Fink, 1989; Kusakabe et al., 1999).

Water concentrations of whole-rock samples, calculated from the amount of H_2 released during isotope analysis, are generally lower than 0.20 wt.% and average at 0.15 wt.%. Two samples contain 0.5-0.6 wt.% water. One is a glassy tephra (34-8) sample from Boleng that also has a relatively high sulfur content of 150 ppm (De Hoog et al., 2001), which suggests that the melt was quenched before degassing was completed. The other water-rich sample is lava from Werung (sample 23-5). δD values do not vary with wt.% H_2O in a systematic way, although values with the highest water contents tend to have slightly higher (less negative) δD values (**Fig. 6**).

3.3.2. Oxygen isotope systematics

Whole-rock $\delta^{18}O$ values exhibit a small range of +5.3 to +6.7‰, with almost 90% of the samples between +5.5 and +6.3‰. Averages of Batur (+5.8±0.3‰) and Soputan (+5.8±0.2‰) do not differ significantly from the overall average (+5.9±0.3‰). Values are slightly higher than $\delta^{18}O$ values for MORB (+5.7 ± 0.2‰, Harmon and Hoefs, 1995), and are in the same range as basaltic to andesitic volcanic bombs from the 1982-83 Galunggung (Java) eruptions (+5.5 to +6.4‰; Harmon and Gerbe, 1993), and basaltic to andesitic lavas from the Banda Arc that are unaffected by crustal assimilation (+5.6 to +6.5‰; Vroon et al., 2001). Considerable

variations exist in whole-rock $\delta^{18}O$ values of both oceanic and continental intraplate basalts as well as in arcs (Harmon and Hoefs, 1995). Our whole-rock values compare also well with the range of arc basalts determined by laser-fluorination measurements of phenocryst (+5.5 to +6.5‰, Eiler et al., 2000; Vroon et al., 2001).

$\delta^{18}O$ values do not vary systematically with H_2O contents of the samples, and only a very weak positive correlation exists between $\delta^{18}O$ and δD (**Fig. 7**). Alteration by meteoric fluids would increase the δD values, but would be accompanied by an increase of $\delta^{18}O$ as well. From the absence of a strong correlation we conclude that the measured δD and $\delta^{18}O$ values reflect magmatic signatures that were not significantly altered by secondary processes.

Lavas from Batur that were erupted successively in 1904, 1905 and 1926 are distinctly higher in both $\delta^{18}O$ and δD relative to other Batur samples, and are also characterized by low contents of SiO_2, K_2O and incompatible trace elements such as Ba, Sr and Zr compared to lavas erupted before and after this period. The comparatively higher $\delta^{18}O$ values are inconsistent with crystal fractionation from isotopically similar magmas, as this would result in higher $\delta^{18}O$ at increasing SiO_2 content (**Fig. 8**). These lavas were most likely derived from separate magma batches, in agreement with observations of Rubin et al. (1989), who invoked the existence of several endmember magmas of different ages and compositions to explain variations in $^{226}Ra/^{230}Th$ of the lavas.

4. Discussion

4.1. Degassing history of Indonesian arc volcanoes

Water contents of primitive arc magmas vary widely, from values as low as 0.3 wt.% for magmas erupted at Galunggung, Indonesia (Sisson and Bronto, 1998) to 6.6 wt.% for Fuego, Guatemala (Sisson and Layne, 1993). Sisson and Grove (1993) and Sobolev and Chaussidon (1996) derived average values of primary water contents of arc magmas between 2 and 4.5 wt.%, and a similar value was obtained in a compilation by Wallace (2005). Parental melts of Batur were estimated to be between 1 and 3 wt.% (Reubi and Nicholls, 2004). Hence, the low

whole-rock water content of our samples indicates that substantial amounts of water have been lost during degassing, which implies that measured δD values are not those of the original, undegassed parental magmas. Fig. 6 shows calculated δD trends corresponding to the degassing of magmas with various initial δD values and 3-5 wt% H_2O.

δD values of two samples (Boleng 34-14 and Werung 23-5; **Fig. 6**) can be explained by closed-system degassing of a magma with an initial δD value of -30 to -25‰, a value insensitive to the initial water content (Section 2.4). However, δD signatures of the remaining samples would be consistent with closed-system degassing only if initial δD values were lower than -50‰, much lower than typical values of -25 to -40‰ for arc magmas (Giggenbach, 1992; Taylor, 1992; Taran et al., 1997; Pineau et al., 1999; Shaw et al., 2008), or if initial water contents were uncommonly high (>6 wt.%). Within-suite variations from Soputan are also inconsistent with closed-system degassing. The sample suite from Soputan spans a short time interval of about 100 years, the lavas show little variation in chemical composition and were erupted during successive events when activity styles remained fairly constant. Therefore, variations in initial δD values and water contents were probably minor and observed within-suite variations in δD values are largely the result of degassing. A rather wide range of δD values is accompanied by moderate variations in H_2O contents (Fig. 6), which is the opposite of which would be observed if degassing had occurred under closed-system conditions.

Open-system degassing results in large isotope shifts in the residual melt. The observed δD signatures of several samples could have been generated by open-system degassing and a minimum initial δD value of -25‰ in combination with initial H_2O contents of less than 3 wt.%. However, for most samples initial δD values close to 0‰ would be required, which is unrealistically high. It is possible that initial water contents were lower, *e.g.*, 1 wt.% (requiring $\delta D = -55‰$). Basalts with such low water contents are known from Galunggung, Indonesia (Sisson and Bronto, 1998) and Medicine Lake, California (Sisson and Layne, 1993), but are the exception rather than the rule for arc basalts (e.g., Sisson and Grove, 1993; Sobolev and Chaussidon, 1996; Wallace, 2005). Higher initial water contents would require even higher initial δD. Single-stage open-system degassing alone is therefore unlikely to be responsible for the observed variations in H_2O contents and δD values in most of the samples.

From these considerations we infer that consecutive stages of closed and open-system degassing constitute a plausible scenario for the isotopic evolution of most of the samples. Starting from initial δD values between -25 and -40‰, most water would be lost under closed-system conditions, and only a very short stage of open-system degassing, starting between ca. 0.35 and 0.7 wt.% H_2O, would be required to explain our data (Fig. 6). The simplest such scenario might be one in which closed-system degassing proceeds in the melt during ascent to a summit holding chamber, followed by essentially open-system type degassing upon eruption. The depth at which the transition from closed to open-system degassing occurs can be estimated from the water content of the samples at that transition, together with the solubility-pressure relationship of mixed H_2O-CO_2 fluids. Using melt H_2O contents of 0.35-0.7 wt.% and plausible estimates of δD_i (-40 to -25‰) and melt CO_2 contents (10-100 ppm), we derive pressures between 15 and 260 bar for the transition from closed to open-system degassing (calculated using VolatileCalc; Newman and Lowenstern, 2002). These low pressures represent depths of several tens to hundreds of meters. Despite the large uncertainties in initial conditions, the conclusion that open-system degassing is syn-eruptive is robust as initial conditions that would lead to pressures compatible with those in shallow magma chambers (>1 kbar), such as $\delta D_i \geq$ -10‰ or CO_2 > 400 ppm at the transition to open-system degassing, are considered uncommon (e.g., Giggenbach, 1992; Holloway and Blank, 2004; Wallace, 2005).

In summary, initial water saturation would have occurred upon depressurization during ascent in which water remained trapped in the melt as bubbles until equilibrating at the pressure of the holding chamber. During ascent the exsolving vapor phase maintained continuous equilibrium with the magma until separation and loss from the magma residing in the holding chamber. Subsequently, upon eruption, vapor would have been removed immediately with little or no isotopic re-equilibration, as evidenced by open-system degassing isotope characteristics. The gas could have been lost to the atmosphere, but open-system behavior can also results from cooling of the magma, which prevents diffusive re-equilibration between water in vesicles and that dissolved in the melt.

A dominant role for closed-system degassing has previously been reported for other basaltic to basaltic-andesitic systems. In a carbon isotope study of gases from Kilauea, Hawaii,

Gerlach and Taylor (1990) concluded that degassing occurred in two stages, an early deep stage and a reservoir-equilibrated stage, both characterized by batch-equilibrium. Degassing at Irazú Volcano (Costa Rica) took place in similar fashion, as melt inclusion H_2O-CO_2 data define a closed-system degassing trend (Benjamin et al., 2007). Degassing was continuous during magma ascent. Volcanic gas data from Stromboli (Italy), representing different styles of eruption, indicate deep closed-system degassing and a transition to open-system degassing at shallow depths where convective overturn of the magma releases the gases (Burton et al., 2007). During larger eruptions, deeper gases with higher CO_2/H_2O ratios are sampled. Similarly, variations in C and H concentrations and isotopic ratios observed in vesicles from submarine lavas pointed to an initial stage of closed-system degassing followed by late-stage open-system degassing (Aubaud et al., 2005). It thus appears that, in many basaltic volcanic systems, exsolved volatiles do not separate from the melt but remain in diffusive equilibrium during ascent, and the Indonesian arc volcanoes in this study are no exception.

4.2. Initial δD values

The δD value of the upper mantle is estimated to be between -70 and -90‰, based on data from primary submarine basalts (around -80‰; Kyser and O'Neill, 1984), obsidians from oceanic islands (-80±4‰; Sheppard and Harris, 1985), and hydrous minerals in mantle xenoliths (mostly -95 to -65‰ but -125‰ for Hawaii; Deloule et al., 1991). In contrast, arc magmas are generally enriched in D (δD = -45 to -25‰; Taylor, 1986, 1992, Giggenbach, 1992; Taran et al., 1997; Pineau et al., 1999, Kusakabe et al., 1999; Shaw et al., 2008), as are high-temperature magmatic gases in arcs (Allard, 1983; Viglino et al., 1985; Taylor, 1986). These isotopic signatures of arc magmas are generally attributed to a D-enriched slab-derived component (Poreda, 1985; Giggenbach, 1992; Taylor, 1992; Taran et al., 1997; Shaw et al., 2008). Possible sources of water include subducted altered oceanic crust, which has an estimated δD value of -60 to -40‰, based on the composition of eclogitized metagabbros from the Alps and Cyclades (Nadeau et al., 1993; Putlitz et al., 2000), and subducted sediments, which have δD values around -30‰ (Giggenbach, 1992). As 'pre-subduction' mantle contains

little water (80-330 ppm; Sobolev and Chaussidon, 1996), the δD values of arc magma sources will be dominated by slab-derived fluids.

As the samples here are strongly degassed we cannot estimate the initial δD values of Indonesian magmas precisely, nor can we detect any significant differences between individual volcanic centers. The values obtained in this study are, however, consistent with a supra-subduction zone mantle enriched in D, as even the degassing scenario with the most limited isotopic shift still requires initial δD values of around -50‰. The presence of a slab-derived fluid component in Indonesian arc magmas is consistent with sulfur isotope data obtained on the same samples, which also suggest such a contribution (De Hoog et al., 2001).

Considering individual volcanic centers in more detail, we observe that the two samples from Boleng can be modeled with a single value for the initial water content and δD, but with contrasting degassing styles (open and closed, respectively, Fig. 6). However, the sample with the open-degassing style has the higher water content, which contradicts our findings that pre-eruptive degassing is mostly closed-system. A similar observation can be made for the two samples from Werung. An alternative interpretation is that all samples were degassed mostly under closed-system conditions but with variable initial δD contents.

The samples from Batur can be divided into two groups with different $\delta^{18}O$ values (Fig. 7). The group with higher $\delta^{18}O$ values also has higher δD values, whereas their water contents are similar. The correlation is surprising as $\delta^{18}O$ is a primary feature of the magmas, whereas δD is largely controlled by the amount and style of degassing. The result could be fortuitous, the high-$\delta^{18}O$ samples being slightly less degassed than the others. More likely, the high $\delta^{18}O$ samples may have had higher initial δD values, which points to a larger influence of the subduction component in these samples, as both high $\delta^{18}O$ and δD values are signatures of the subducted slab component (Giggenbach, 1992; Eiler et al., 2000).

5. Conclusions

We developed a model for hydrogen isotope changes in degassing magma that takes the variation of water species with water content and temperature into account. In combination with existing experimental data, we infer that the fractionations between OH∗ and H_2O in

hydrous melt and exsolved vapor (H_2O) can be expressed as $10^3 \ln \alpha_{OH*}$ for basalts is $35.0 + 16.7 \times 10^6/T^2$ and $10^3 \ln \alpha_{H_2O*}$ is $-29.9 + 16.7 \times 10^6/T^2$, respectively. The influence of temperature on the bulk fractionation factor is of minor importance under magmatic conditions.

Whole-rock hydrogen isotope compositions of basalts and basaltic andesites from Indonesian arc volcanoes range between -109 and -57‰, although most values fall between -100 and -80‰. We infer a two-stage degassing scenario, whereby, during ascent to and storage in a shallow reservoir, degassing proceeds under closed-system conditions, while subsequent eruptive degassing is characterized by open-system behavior. Our data point to the presence of predominantly slab-derived water in the sources of Indonesian magmas, consistent with inferences for other arc systems. Considering the limited spread in observed δD values, degassing mechanisms in the investigated basaltic volcanic centers are remarkably uniform.

Acknowledgements

References

Allard. P., 1983. The origin of hydrogen, carbon, sulfur, nitrogen and rare gases in volcanic exhalations: evidence from isotope geochemistry. In: Tazieff, H., Sabroux, J.C. (Eds), Forecasting volcanic events. Elsevier, Amsterdam, pp. 337-386.

Anderson, S.W., Fink., J.H., 1989. Hydrogen-isotope evidence for extrusion mechanisms of the Mount St Helens lava dome. Nature 341: 521-523.

Aubaud, C., Pineau, F., Hékinian, R., Javoy, M., 2005. Degassing of CO_2 and H_2O in submarine lavas from the Society hotspot, Earth and Planetary Science Letters, 235, 511-527.

Behrens, H., Novak., M., 2003. Quantification of H2O speciation in silicate glasses and melts by IR spectroscopy – in situ versus quench techniques. Phase Transactions 76, 45-61.

Benjamin, E.R., Plank, T., Wade, J.A., Kelley, K.A., Hauri, E.H., Alvarado, G.E., 2007. High water contents in basaltic magmas from Irazú Volcano, Costa Rica. Journal of Volcanology and Geothermal Research 168, 68-92.

Bigeleisen, J., Perlman, M.L., Prosser, H.C., 1952. Conversion of hydrogenic materials to hydrogen for isotopic analysis. Analytical Chemistry 24: 1356-1357.

Botcharnikov, R.E., Behrens, H., Holtz, F., 2006. Solubility and speciation of C-O-H fluids in andesitic melt at T=1100-1300°C and P=200 and 500MPa. Chemical Geology 229, 125-143

Burton, M., Allard, P., Muré, F., La Spina, A., 2007. Magmatic gas composition reveals the source depth of slug-driven strombolian explosive activity. Science 317, 227-230.

Clayton, R.N., Mayeda, T., 1963. The use of bromine pentaXuoride in the extraction oxygen from oxides and silicates for isotopic analysis. Geochimica et Cosmochimica Acta 27, 43-52.

De Hoog. J.C.M., Taylor, B.E., Van Bergen, M.J., 2001. Sulfur isotope systematics of Indonesian arc basalts and implications for the sulfur cycle in subduction zones. Earth and Planetary Science Letters189: 237-252.

Deloule, E., Albarède, F., Sheppard, S.M.F., 1991. Hydrogen isotope heterogeneities in the mantle from ion probe analysis of amphiboles from ultramafic rocks. Earth and Planetary Science Letters105, 543-553.

Dingwell, D.B., Webb, S.L., 1990. Relaxation in silicate melts. Eur. J. Mineral. 2: 427-449.

Dobson, P.F., Epstein, S., Stolper, E.M., 1989. Hydrogen isotope fractionation between coexisting vapor and silicate glasses and melts at low pressure. Geochimica et Cosmochimica Acta 53, 2723-2730.

Driesner, T., 1997. The effect of pressure on deuterium-hydrogen fractionation in high-temperature water. Science 277, 791-794

Eiler, J.M., Crawford, A., Elliott, T., Farley, K.A., Valley, J.W., Stolper, E.M., 2000. Oxygen isotope geochemistry of oceanic-arc lavas. Journal of Petrology 41, 229-256.

Gerlach, T.M., Taylor, B.E., 1990. Carbon isotope constraints on degassing of carbon dioxide

from Kilauea Volcano. Geochimica et Cosmochimica Acta 54, 2051-2058

Giggenbach, W.F., 1992. Isotopic shifts in waters from geothermal and volcanic systems along convergent plate boundaries and their origin. Earth and Planetary Science Letters 113, 495-510

Hamilton, W., 1979. Tectonics of the Indonesian region. U.S.G.S. Prof. Paper 1078, 345 p.

Harmon, R.S., Gerbe, M.-C., 1992. The 1982-1983 eruption at Galunggung Volcano, Java, Indonesia : Oxygen isotope geochemistry of a chemically zoned magma chamber. Journal of Petrology 33, 585-609.

Harmon, R.S., Hoefs, J., 1995. Oxygen isotope heterogeneity of the mantle deduced from global ^{18}O systematics of basalts from different geotectonic settings. Contributions to Mineralogy and Petrology 120, 95-114.

Holloway, J.R., Blank, J.G., 1994. Application of experimental results to C-O-H species in natural melts. In: M.R. Carroll MR, J.R. Holloway JR (Eds.), Volatiles in magmas. Reviews in Mineralogy 30, 281-330.

Hoogewerff, J.A., 1999. Magma genesis and slab-wedge interaction across an island arc-continent collision zone, East Sunda Arc, Indonesia. PhD thesis, Utrecht University, Geologica Ultraiectina 178, 199 p.

Horita, J., Driesner, T., Cole, D.R., 1999. Pressure effect on hydrogen isotope fractionation between brucite and water at elevated temperatures. Science 286, 1545-1547.

Hui, H., Zhang, Y., Xu, Z., Behrens, H., 2008. Pressure dependence of the speciation of dissolved water in rhyolitic melts. Geochimica et Cosmochimica Acta 72, 3229-3240.

IAEA, 2001. GNIP Maps and Animations. International Atomic Energy Agency, Vienna. Accessible at http://isohis.iaea.org

Ihinger, P.D., Zhang, Y., Stolper, E.M., 1999. The speciation of dissolved water in rhyolitic melt. Geochimica et Cosmochimica Acta 63, 3567-3578.

Kuroda, Y., Hariya, Y., Suzuoki, T., Matsuo, S., 1982. D/H fractionation between water and the melts of quartz, K-feldspar, albite and anorthite at high temperature and pressure. Geochemical Journal 16, 73-78.

Kusakabe, M., Sato, H., Nakada, S., Kitamure, T., 1999. Water contents and hydrogen isotopic ratios of rocks and minerals from the 1991 eruption of Unzen volcano, Japan. Journal of Volcanology and Geothermal Research 89, 231-242.

Kyser, T.K., O'Neill, J.R., 1984. Hydrogen isotope systematics of submarine basalts. Geochimica et Cosmochimica Acta 48, 2123-2133.

Liu, Y., Behrens, H., Zhang, Y., 2004. The speciation of H_2O in dacitic melt. American Mineralogist 89, 277-284.

Nadeau, S., Philippot, P., Pineau, F., 1993. Fluid inclusion and mineral isotopic compositions (H-C-O) in eclogitic rocks as tracers of local fluid migration during high-pressure metamorphism. Earth and Planetary Science Letters 114, 431-448.

Newman, S., Epstein, S., Stolper, E.M., 1988. Water, carbon dioxide, and hydrogen isotopes in glasses from the ca. 1340 A.D. eruption of the Mono Craters, California: constraints on degassing phenomena and initial volatile content. Journal of Volcanology and Geothermal Research 35, 75-96.

Newman, S., Lowenstern, J.B., 2002. VOLATILECALC: a silicate melt-H_2O-CO_2 solution model written in Visual Basic for Excel, Computers and Geosciences 28, 597- 604.

Nowak, M., Behrens, H., 1995. The speciation of water in haplogranitic glasses and melts determined by in situ near-infrared spectroscopy. Geochimica et Cosmochimica Acta 59, 3445-3450.

Nowak, M., Behrens, H., 2001. Water in rhyolitic magmas: getting a grip on a slippery problem. Earth and Planetary Science Letters 184, 515-522.

Ohlhorst, S., Behrens, H., Holtz, F., 2001. Compositional dependence of molar absorptivities of near-infrared OH- and H_2O bands in rhyolitic to basaltic glasses. Chemical Geology 174, 5-20.

Pineau, F., Shilobreeva, S., Kadik, A., Javoy, M., 1998. Water solubility and D/H fractionation in the system basaltic andesite-H_2O at 1250°C and between 0.5 and 3 kbars. Chemical Geology 147, 173-184.

Pineau, F., Semet, M.P., Grassinaeu, N., Okrugin, V.M., Javoy, M., 1999. The genesis of the stable isotope (O, H) record in arc magmas: the Kamchatka's case. Chemical Geology 135, 93-124.

Poreda, R.., 1985. Helium-3 and deuterium in back-arc basalts: Lau Basin and the Mariana Through. Earth and Planetary Science Letters 73, 244-254.

Putlitz, B., Matthews, A., Valley, J.W., 2000. Oxygen and hydrogen isotope study of high-pressure metagabbros and metabasalts (Cyclades, Greece): implications for the subduction of oceanic crust. Contributions to Mineralogy and Petrology 138, 114-126.

Reubi, O., Nicholls, I.A., 2004. Magmatic evolution at Batur volcanic field, Bali, Indonesia: petrological evidence for polybaric fractional crystallization and implications for caldera-forming eruptions. Journal of Volcanology and Geothermal Research 138, 345-369.

Richet, P., Roux, J., Pineau, F., 1986. Hydrogen isotope composition in the system H_2O-liquid $NaAlSi_3O_8$: new data and comments on D/H fractionation in hydrothermal experiments. Earth and Planetary Science Letters 78, 115-120.

Rubin, K.H., Wheller, G.E., Tanzer, M.O., MacDougall, J.D., Varne, R., Finkel, R., 1989. [238]U decay series systematics of young lavas from Batur volcano, Sunda Arc. Journal of Volcanology and Geothermal Research 38, 215-226.

Schmidt, B.C., Riemer, T., Kohn, S.C., Behrens, H., Dupree, R., 2000. Different water solubility mechanisms in hydrous glasses along the Qz-Ab join: evidence from NMR spectroscopy. Geochimica et Cosmochimica Acta 64, 513-526.

Shaw, A.M., Hauri, E.H., Fischer, T.P., Hilton, D.R., Kelley, K.A., 2008. Hydrogen isotopes in Mariana arc melt inclusions: Implications for subduction dehydration and the deep-Earth water cycle. Earth and Planetary Science Letters 275, 138-145.

Shen, A., Keppler, H., 1995. Infrared spectroscopy of hydrous silicate melts to 1000ºC and 10 kbar: direct observation of H_2O speciation in a diamond-anvil cell. American Mineralogist 80, 1335-1338.

Sheppard, S.M.F., Harris, C., 1985. Hydrogen and oxygen isotope geochemistry of Ascension Island lavas and granites: variation with crystal fractionation and interaction with sea water. Contributions to Mineralogy and Petrology 91, 74-81

Silver, L.A., Stolper, E.M., 1989. Water in albitic glasses. Journal of Petrology 30, 667-709

Silver, L.A., Ihinger, P.D., Stolper, E.M., 1990. The influence of bulk composition on the speciation of water in silicate glass. Contributions to Mineralogy and Petrology 104, 142-162.

Sisson, T.W., Bronto, S., 1998. Evidence for pressure-release melting beneath magmatic arcs from basalt at Galunggung, Indonesia. Nature 391, 883-886.

Sisson, T.W., Grove, T.L., 1993. Temperatures and H_2O contents of low-MgO high-alumina basalts. Contributions to Mineralogy and Petrology 113, 167-184.

Sisson, T.W., Layne, G.D., 1993. H_2O in basalt and basaltic andesite glass inclusions from four subduction-related volcanoes. Earth and Planetary Science Letters 117, 619-635.

Sobolev, A.V., Chaussidon, M., 1996. H_2O concentrations in primary melts from supra-subduction zones and mid-ocean ridges: implications for H_2O storage and recycling in the mantle. Earth and Planetary Science Letters 137, 45-55.

Stolper, E.M., 1982a. Water in silicate melts: an infrared spectroscopic study. Contributions to Mineralogy and Petrology 81, 1-17.

Stolper, E.M., 1982b. The speciation of water in silicate melts. Geochimica et Cosmochimica Acta 46, 2609-2620.

Stolper, E.M., 1989. Temperature dependence of the speciation of water in rhyolitic melts and glasses. American Mineralogist 74, 1247-1257.

Taran, Y.A., Pokrovsky, B.G., Volynets, O.N., 1997. Hydrogen isotopes in hornblendes and biotites from Quaternary volcanic rocks of the Kamchatka-Kurile arc. Geochemical Journal 31, 203-221.

Taylor, B.E., 1986. Magmatic volatiles: isotopic variation of C, H, and S. In: Valley, J.W., Taylor, H.P. O'Neil, J.R. (Eds.), Stable isotopes in high temperature geological processes. Reviews in Mineralogy 16, 185-225.

Taylor, B.E., 1991. Degassing of Obsidian Dome rhyolite, Inyo volcanic chain, California. In: Taylor, H.P. Jr., O'Neil, J.R., Kaplan, I.R. (Eds.), A tribute to Samuel Epstein, Geochemical Society, Special Publublication No. 3, 339-353.

Taylor, B.E., 1992. Degassing of H_2O from rhyolitic magma during eruption and shallow intrusion, and the isotopic composition of magmatic water in hydrothermal systems. In: Hedenquist, J.K. (Ed.), Magmatic contributions to hydrothermal systems and the behavior of volatiles in magma. Geological Survey of Japan, Report 279, 190-194.

Taylor, B.E., Westrich, H.R., 1985. Hydrogen isotope exchange and water solubility in experiments using natural rhyolite obsidian (abstract). EOS 66, p. 387.

Taylor, B.E., Eichelberger, J.C., Westrich, H.R., 1983. Hydrogen isotopic evidence of rhyolitic magma degassing during shallow intrusion and eruption. Nature 306, 541-545

Viglino, J.A., Harmon, R.S., Borthwick, J., Nehring, N.L., Motyka, R.J., White, L.D., Johnston, D.A., 1985. Stable-isotope evidence for a magmatic component in fumarole condensates from Augustine volcano, Cook inlet, Alaska, U.S.A. Chemical Geology 49, 141-157.

Vroon, P.Z., Lowry, D., Van Bergen, M.J., Boyce, A.J., Mattey, D.P, 2001. Oxygen isotope systematics of the Banda Arc: low $\delta^{18}O$ despite involvement of subducted continental material in magma genesis. Geochimica et Cosmochimica Acta 65, 589-609.

Wallace, P.J., 2005. Volatiles in subduction zone magmas: concentrations and fluxes based on melt inclusion and volcanic gas data. Journal of Volcanology and Geothermal Research 140, 217-240.

Wilding, M.C., MacDonald, R., Davies, J.E., Fallick, A.E., 1993. Volatile characteristics of peralkaline rhyolites from Kenya: an ion-microprobe, infrared spectroscopic and hydrogen isotope study. Contributions to Mineralogy and Petrology 114, 264-275.

Withers, A.C. , Zhang, Y., Behrens, H., 1999. Reconciliation of experimental results on H_2O speciation in rhyolitic glass using in-situ and quenching techniques. Earth and Planetary Science Letters 173, 343-349.

Zeng, Q., Neksavil, H., Grey, C.P., 2000. In support of a depolymerization model for water in aluminosilicate glasses: information from NMR spectroscopy. Geochimica et Cosmochimica Acta 64, 883-896.

Zhang, Y, 1999. H_2O in rhyolitic glasses and melts: measurement, speciation, solubility, and diffusion. Reviews of Geophysics 37, 493-516.

Zhang, Y., Stolper, E.M., Ihinger, P.D., 1995. Kinetics of reaction $H_2O + O = 2OH$ in rhyolitic glasses: preliminary results. American Mineralogist 80, 593-612.

Figure captions

Fig. 1 Variation of C_{OH*} and C_{H_2O*} (in wt.%) with total water concentration (in wt.%) at 500, 800 and 1100°C in rhyolitic melt calculated for ideal and regular solution models using fit parameters by Ihinger et al. (1997).

Fig. 2 Plot of $10^3 \ln \alpha$ against T^{-2} for various hydrous minerals (closed triangles) and water-poor feldspathic and rhyolitic glasses (obsidian: closed diamonds; after Dobson et al., 1989). The lines for basaltic to andesitic melts derived from our fractionation model are shown separately for water dissolved as OH* and H_2O* (Eq. 6 and 7, respectively). Also plotted are data from Pineau et al. (1998) (half filled circles) for basaltic andesite including respective water contents. $10^3 \ln \alpha_{v-m}$ decreases with increasing water content because of the relative increase of H_2O* at the expense of OH*. The open circle indicates the value of $10^3 \ln \alpha_{v-m}$ for a hypothetical water content of 0 wt% H_2O, extrapolated from the data of Pineau et al. (1998) to calculate $\alpha_{vapor-OH*}$. The small open square represents melt-rhyolite fractionation factor from an experiment by Taylor and Westrich (1985) at 50 MPa, equivalent to ca. 2.3 wt.% water.

Fig. 3 Variation of $\Delta D_{vapor-melt}$ (‰) with total water content (in wt.%) derived from experimental data of Pineau et al. (1998) for basaltic andesite melt at 1250°C (open diamonds) and the water speciation model by Ihinger et al. (1999). These data have been used to derive values for $\alpha_{vapor-H_2O*}$ and $\alpha_{vapor-OH*}$ of 0.9775 and 1.0431, respectively. Note that a value of $\alpha_{vapor-H_2O*} = 1$ does not fit the experimental data of Pineau et al. (1998). Also indicated are curves for 950°C and our simplified temperature-independent model (Eq. 13), showing that temperature effects on $\Delta D_{vapor-melt}$ are relatively small.

Fig. 4   Open and closed-system degassing model curves for constant (dashed lines) and variable fractionation factors according to our hydrogen fractionation model (continuous lines) in a δD (‰) - log H_2O (wt.%) diagram for an initial water content of the melt of 5 wt.%. Values of constant vapor melt isotopic fractionation factors are indicated with numbers, the variable fractionation factors vary between the two indicated extremes. The set of open-system degassing curves represents different temperatures (900-1250°C), but are virtually indistinguishable. Dotted lines show the effect of lower initial water content of 2 wt.% on the degassing curves.

Fig. 5   Tectonic map of the Indonesian arc system (after Hamilton, 1979) indicating the locations of seven volcanoes investigated in this study.

Fig. 6 δD (‰) - H_2O (wt.%) variation diagram showing the compositions of the Indonesian samples and modeled degassing lines for open (dashed line), closed (continuous line) and two-stage degassing (dashed dotted line) for a range of initial conditions indicated by numbers (initial water content / initial δD values). Fractionation factors were calculated using the model presented in Section 2.4 (Eq. 12).

Fig. 7   Variation of δD (‰) vs. $\delta^{18}O$ (‰) of the Indonesian samples. Dashed ellipses indicate two groups for Batur that probably represent different magma batches with different initial $\delta^{18}O$ and possibly δD values. Inset shows same diagram on expanded scale. Grey field represents "andesitic waters" from □Giggenbach (1992). Straight dotted lines parallel to the meteoric water line indicate the composition of secondary minerals in equilibrium with meteoric water at increasingly lower temperatures from left to right. Local meteoric water data from IAEA (2001).

Fig. 8   Variation diagram of SiO_2 (wt.%) vs. $\delta^{18}O$ (‰) for Indonesian arc basalts. The effects of fractional crystallization and low-T alteration (indicated by arrows) are small in these samples. Note that the two groups of Batur samples (marked by dashed ellipses) cannot be related by fractional crystallization or low-T alteration, which suggests that they originate from different magma batches.

Table 1. Sample descriptions, whole-rock SiO_2 and K_2O contents, loss on ignition (LOI), water contents and H, O isotope compositions of samples from this study

| volcano	sample	eruption date	description	SiO_2 wt%	K_2O wt%	LOI wt%	H_2O wt%	δD ‰	$\delta^{18}O$ ‰
Krakatau	KR1	1995	scoria bomb	55.1	0.97	0.0	0.17	-98	+5.4
Guntur	GU3	historic	lava flow	51.6	0.53	-0.2	0.14	-85	+5.7
	GU5-I [a]	historic	lava flow	56.5	1.23	0.0	0.12	-109	+6.3
	GU5-II [a]						0.13	-101	+5.9
Batur	BR2	1904	lava flow	51.9	1.01	-0.2	0.18	-83	+6.2
	BR3	1974	lava flow	53.1	1.18	-0.2	0.15	-99	+5.7
	BR4	1963	lava flow	53.5	1.20	-0.1	0.14	-93	+5.7
	BR5 [b]	1994	scoria bomb	53.3	1.23	-0.2	0.14	-100	+5.9
	BR7	1926	lava flow	51.7	1.01	-0.2	0.16	-88	+6.1
	BR8	1905	lava flow	51.4	0.94	-0.2	0.15	-80	+6.2
	BR9	1968	lava flow	53.2	1.19	-0.2	0.13	-94	+5.5
	BR10	1888	lava flow	54.4	1.29	-0.1	0.18	-90	+5.5
	BR11	1849	lava flow	54.4	1.32	-0.1	0.18	-96	+5.7
	BR12 [b]	1994	scoria bomb	53.5	1.23	-0.3	0.12	-94	+5.8
Rinjani	RI3.1 [c]	1943	blocky lava flow	54.5	1.78	0.0	0.12	-101	+6.5
	RI3.2 [c]	1943	blocky lava flow	54.0	1.71	0.0	0.14	-101	+6.1
Boleng	34-8	historic	pumice fall	53.1	1.47	0.3	0.57	-74	+6.0
	34-14	historic	lava flow	50.3	1.49	-0.3	0.24	-57	+6.3
Werung	23-2	historic	lava flow	53.0	0.41	-0.3	0.08	-64	n.a.
	23-5	historic	lava flow	51.5	0.31	0.6	0.55	-61	+6.7
Lewotolo	17-3	historic	lava flow	47.2	1.46	-0.2	0.08	-92	+5.3
	17-4	historic	lava flow	48.9	1.84	-0.1	0.05	-98	+5.8
Soputan	SP1	~1900	lava flow	49.6	0.31	-0.5	0.11	-83	+5.7
	SP2	~1900	lava flow	49.4	0.31	-0.5	0.10	-84	+5.6
	SP3	~1900	lava flow	49.9	0.29	-0.5	0.07	-93	+5.5
	SP4	~1900	lava flow	50.3	0.29	-0.5	0.07	-87	+6.0
	SP5	1994	dome lava	49.6	0.28	-0.6	0.05	-88	+5.6
	SP6	1995	lava flow	49.8	0.29	-0.5	0.05	-84	+6.1
	SP7	1994	dome lava	50.1	0.29	-0.5	0.05	-94	+6.0
	SP13	1966	lava flow	50.6	0.30	-0.6	0.07	-98	+5.5

Oxides and LOI in wt.%, normalized to 100 wt.%, analyzed by XRF. Major-element compositions and LOI of Boleng, Werung and Lewotolo samples from Hoogewerff (1999), others from De Hoog et al. (2001). δD in permil relative to V-SMOW, precision is 2‰. $\delta^{18}O$ in permil relative to V-SMOW, precision is 0.2‰ [a] Two aliquots of the same powdered sample processed separately in Kiba extraction. [b] Two scoria bombs from same eruption. [c] Two samples from same flow sampled ten meters apart.
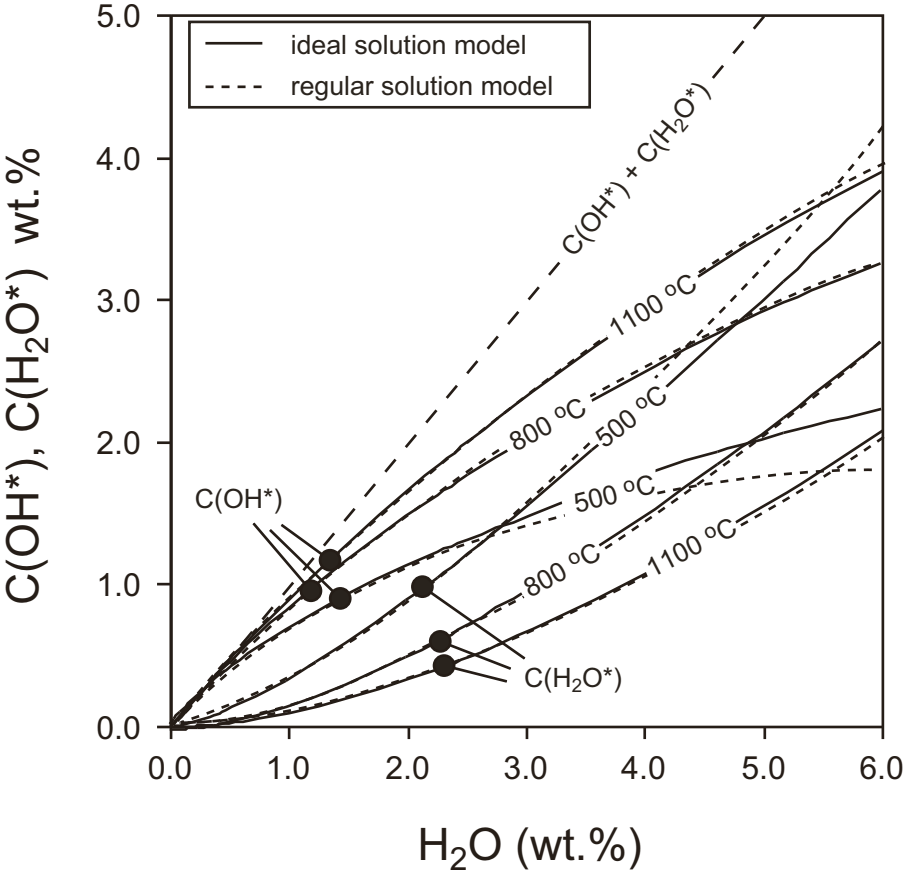
De Hoog et al. Figure 1
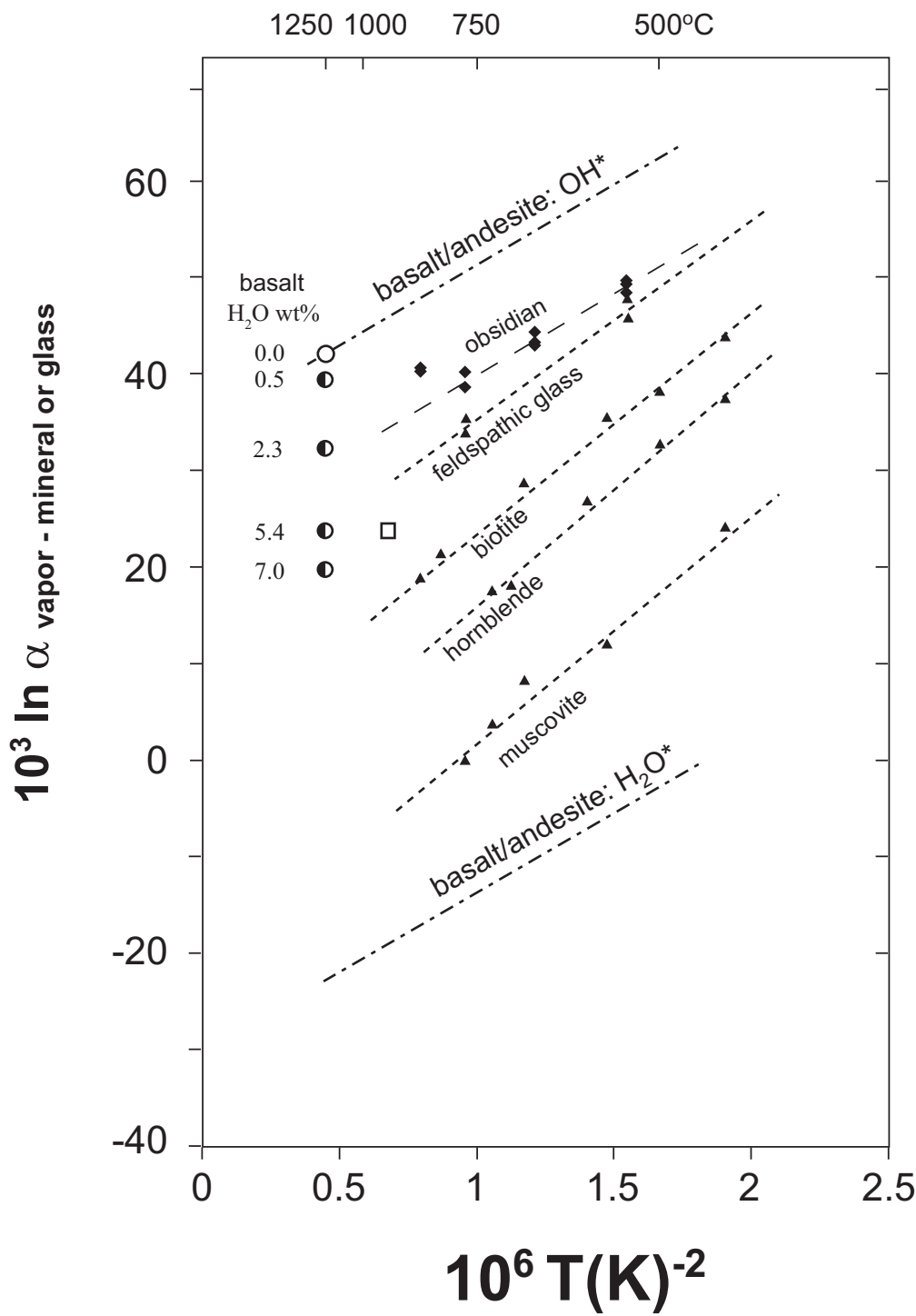
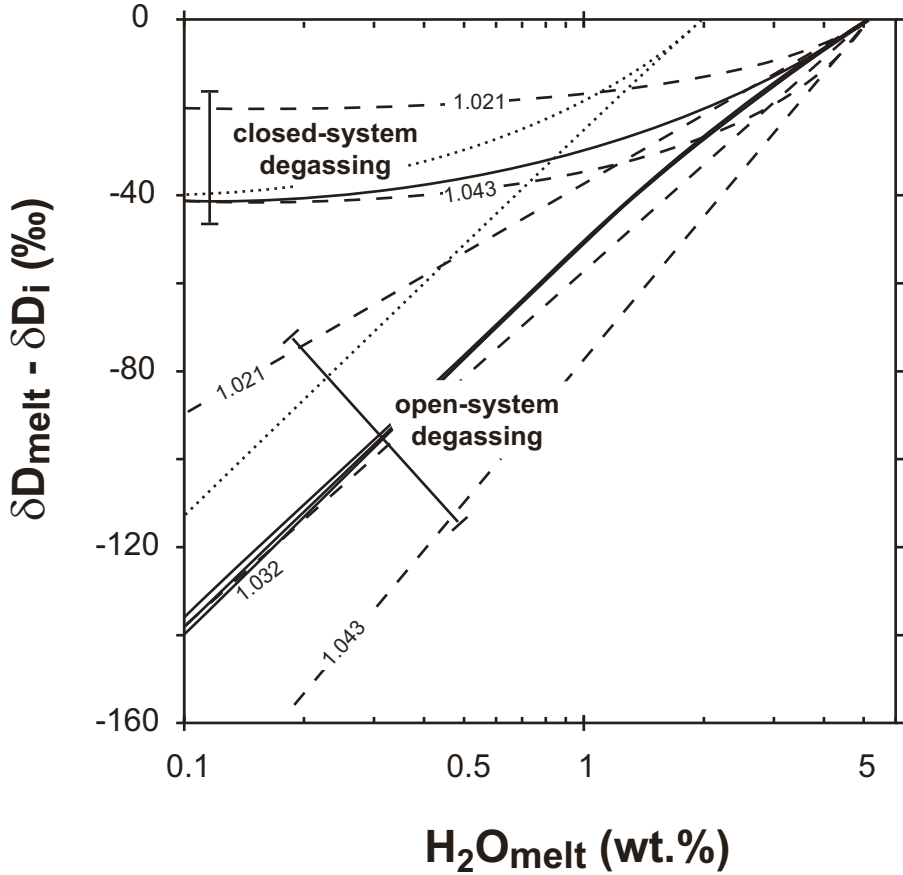De Hoog et al. Figure 2
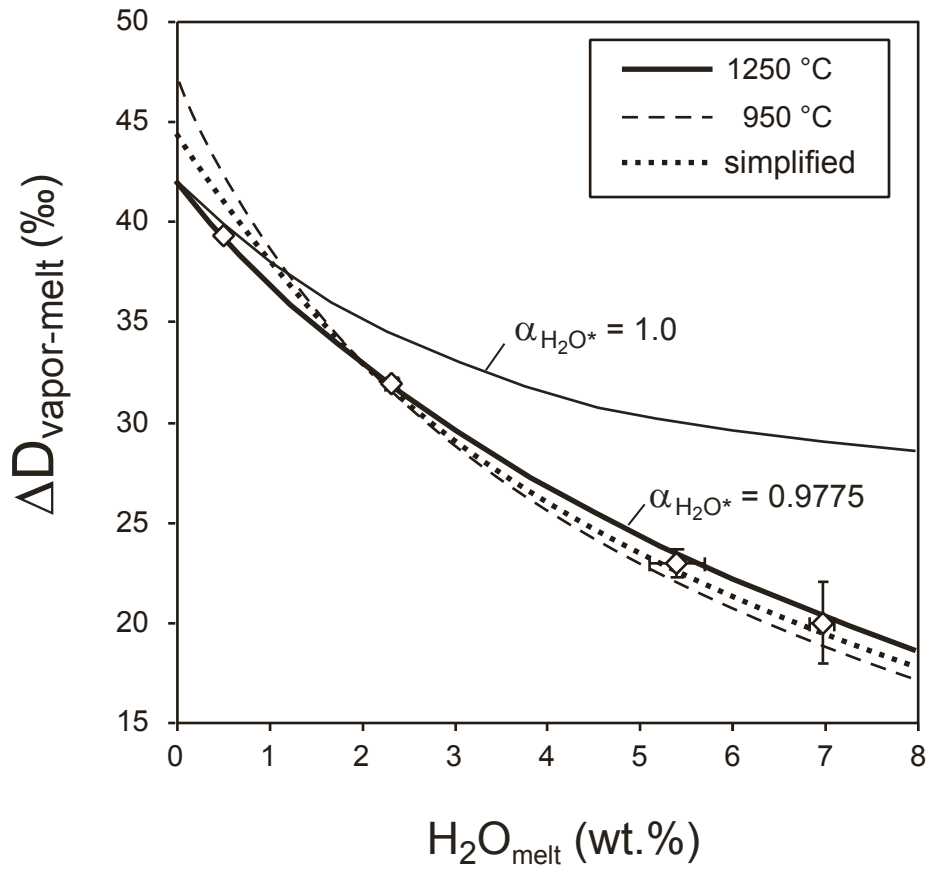
De Hoog et al. Figure 3
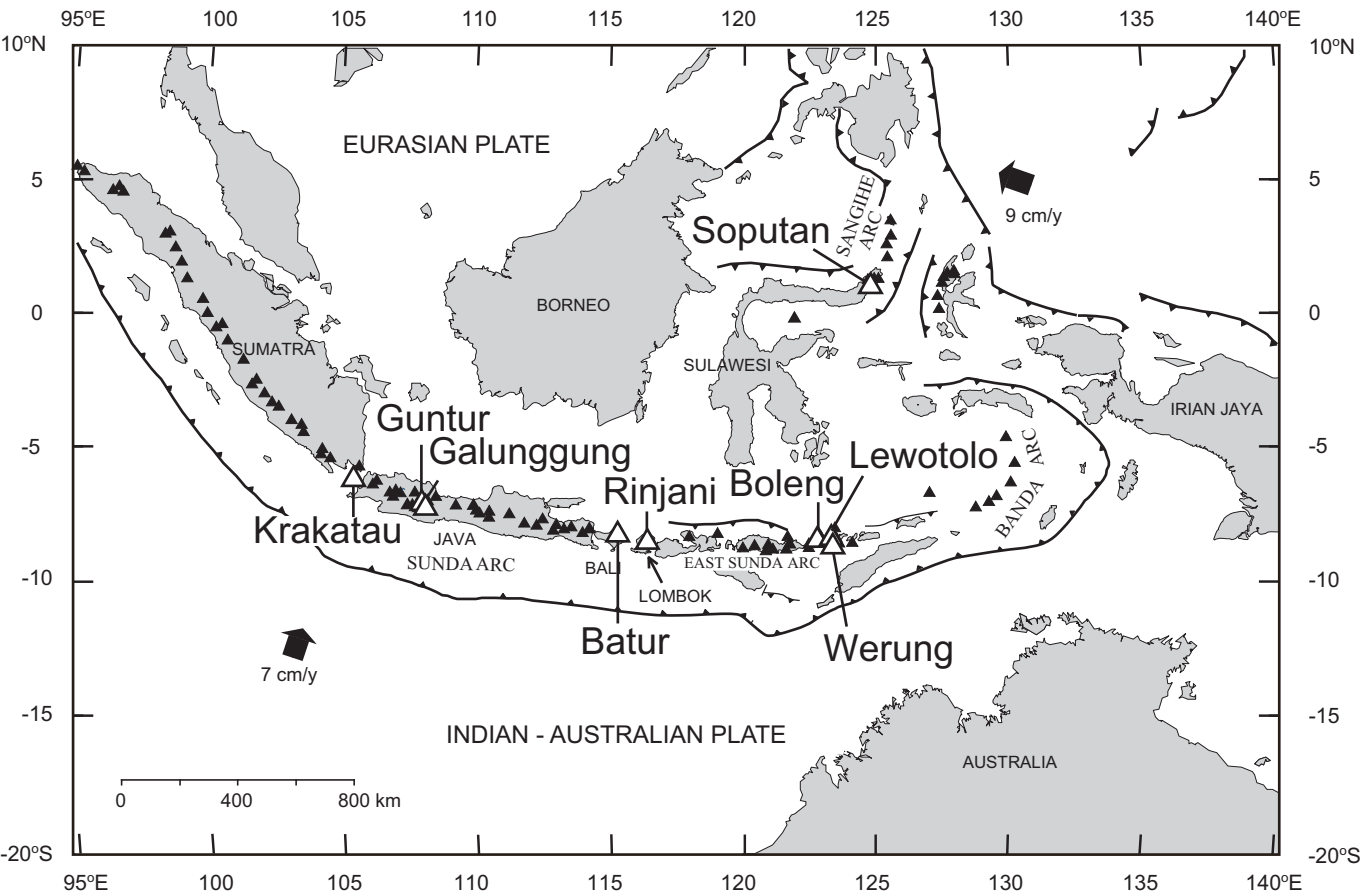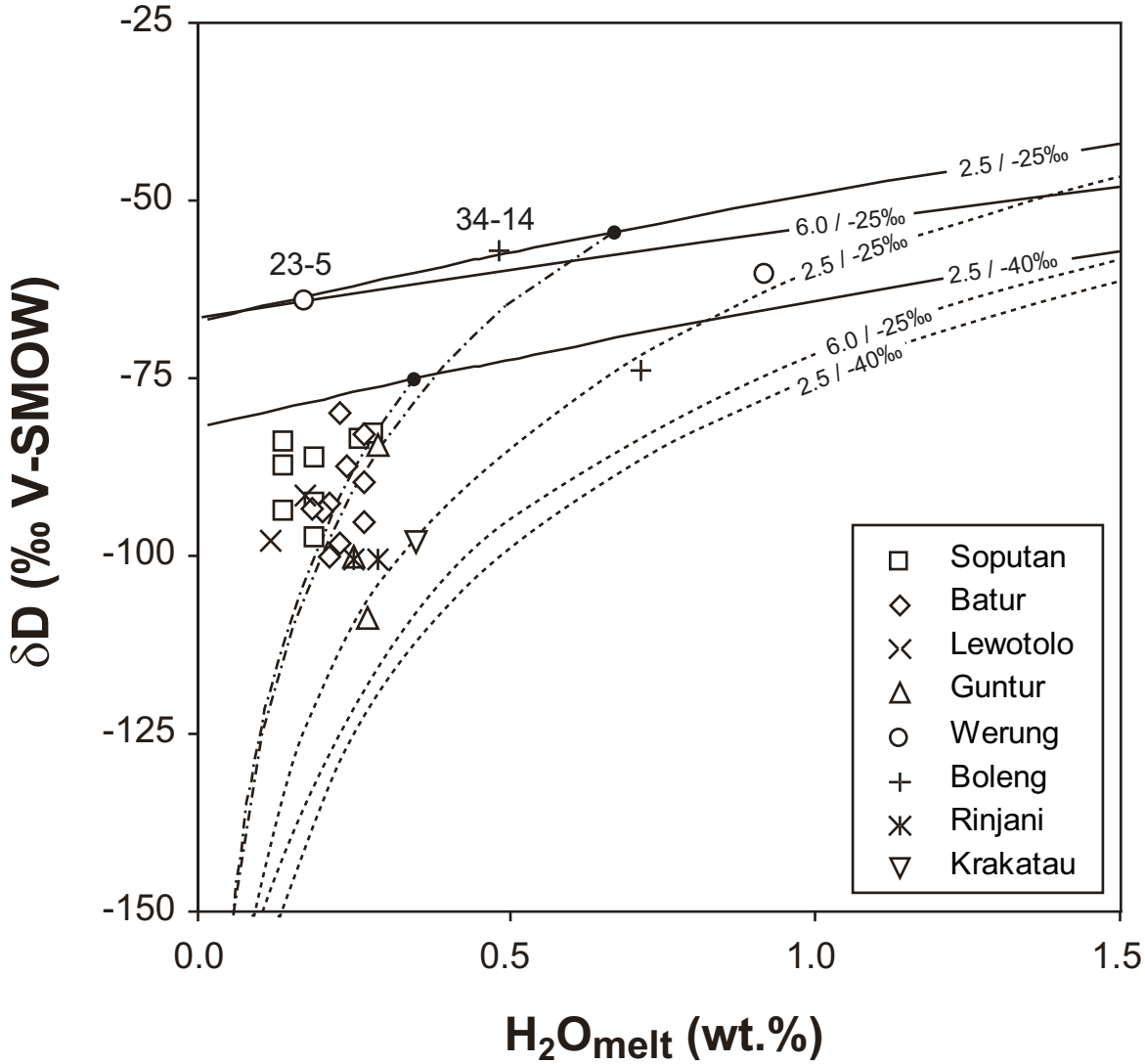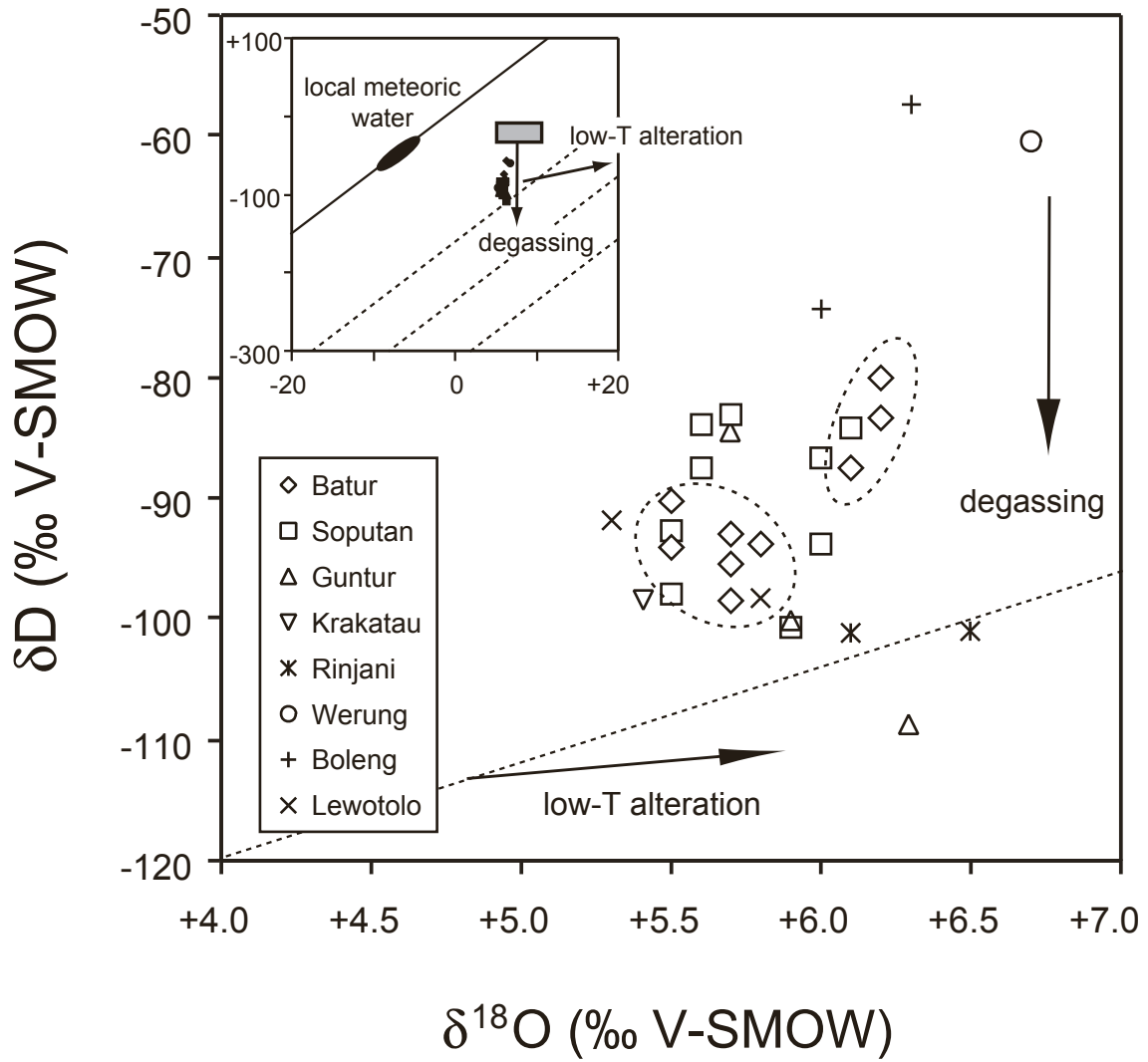
Figure 4. De Hoog et al.

Figure 5. De Hoog et al.

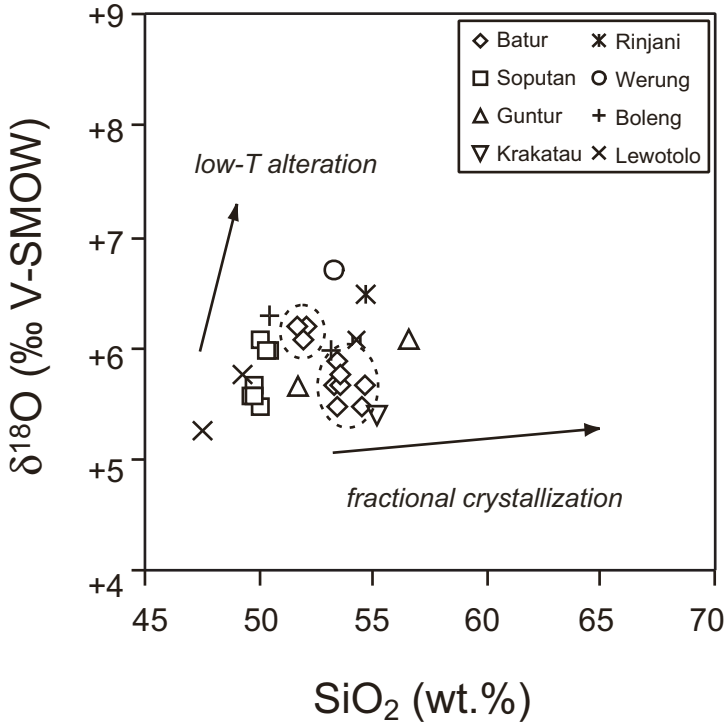Figure 6. De Hoog et al.

Fig. 7. De Hoog et al.

Fig. 8. De Hoog et al.